V European Conference on Computational Fluid Dynamics
ECCOMAS CFD 2010
J. C. F. Pereira and A. Sequeira (Eds)
Lisbon, Portugal,14-17 June 2010

SOLVING THE MULTI-LAYER SHALLOW WATER EQUATIONS USING THE FINITE VOLUME MODIFIED METHOD OF CHARACTERISTICS

F. Benkhaldoun* and **M. Seaid†**

*LAGA, Université Paris 13
99 Av J.B. Clement, 93430 Villetaneuse, France
e-mail: fayssal@math.univ-paris13.fr
†School of Engineering and Computing Sciences, University of Durham
South Road, Durham DH1 3LE, UK
e-mail: m.seaid@durham.ac.uk

Key words: Multi-layer shallow water equations, Finite volume schemes, Method of characteristics, Wind-driven flows

Abstract. *A new finite volume method is proposed for numerical solution of multi-layer shallow water equations on non-flat topography. The equations include the wind shear stresses on the water free-surface and bed frictions on the bottom topography. The layers can be formed in the shallow water model based on the variation of water density which depend on the water temperature and salinity. For a water body with equal density the model reduces to the canonical single-layer shallow water equations. The multi-layer shallow water equations form a system of conservation laws with source terms for which the computation of the eigenvalues is not trivial. For most practical applications, complex eigenvalues can arise in the system and the multi-layer shallow water equations is not hyperbolic any more. This property make the application of conventional finite volume methods difficult even impossible for those methods which require in their formulation the explicit computation of the eigenvalues. In the current study, we propose a new finite volume method that avoids the solution of Riemann problems. At each time step, the method consists of two stages to update the new solution. In the first stage, the multi-layer shallow water equations are rewritten in a non-conservative form and the intermediate solutions are calculated using the modified method of characteristics. The characteristic curves are computed for each layer using the velocity field associated with each layer. The intermediate solutions are obtained by interpolation at the departure points. In the second stage, the numerical fluxes are reconstructed from the intermediate solutions in the first stage and used in the conservative form of the multi-layer shallow water equations. The proposed method avoids Riemann problem solvers, satisfies the conservation property and suitable for multi-layer shallow water equations on non-flat topography. Numerical results are presented for a two-layer wind-driven shallow water flow. The obtained results for different wind conditions are considered to be representative, and might be helpful for a fair rating of finite volume solution schemes, particularly in long time computations.*

1 INTRODUCTION

Mathematical modelling of tidal flows in water systems is based on the formulation and solution of the appropriate equations of continuity and motion of water. In general, tidal flows represent a three-dimensional turbulent Newtonian flow in complicated geometrical domains. The costs of incorporating three-dimensional data in natural water courses is often excessively high. Computational efforts needed to simulate three-dimensional turbulent flows can also be significant. In view of such considerations, many researchers have tended to use rational approximations in order to develop two-dimensional hydrodynamical models for shallow water flows. Indeed, under the influence of gravity, many free-surface water flows can be modelled by the shallow water equations with the assumption that the vertical scale is much smaller than any typical horizontal scale. These equations can be derived from the depth-averaged incompressible Navier-Stokes equations using appropriate free-surface and boundary conditions along with a hydrostatic pressure assumption. The shallow water equations in depth-averaged form have been successfully applied to many engineering problems and their application fields include a wide spectrum of phenomena other than water waves. For instance, the shallow water equations have applications in environmental and hydraulic engineering, for example, for tidal flows in an estuary or coastal regions, rivers, reservoir and open channel flows. Such practical flow problems are not trivial to simulate since the geometry can be complex and the topography irregular. However, single-layer shallow water equations have the drawback of missing some physical dynamics in the vertical motion. Therefore, during the last decades, multi-layer shallow water models have been attracted more attention and have became a very useful tools to solve hydrodynamical flows such as rivers, estuaries, bays and other nearshore regions where water flows interact with the bed geometry and wind shear stresses, see for instance [7, 5, 4, 6, 9]. The main advantage of these models is the fact that the multi-layer shallow water model avoids the expensive three-dimensional NavierStokes equations and obtains stratified horizontal flow velocities as vertical velocities are relatively small and the flow is still within the shallow water regime.

Numerical treatment of the multi-layer shallow water equations often presents difficulties due to their nonlinear form, presence of the advective term, coupling between the free-surface equation and the equations governing the water flow, compare [5, 4, 6, 9] among others. In addition, the difficulty in these models comes from the coupling terms involving some derivatives of the unknown physical variables that make the system non-conservative and eventually non-hyperbolic. Due to these terms, a numerical scheme originally designed for single-layer shallow water equations will lead to instabilities when it is applied to each layer separately. In the present work we propose a new finite volume modified method of characteristics to solve the multi-layer shallow water equations. The method avoids the solution of Riemann problems and belongs to the predictor-corrector type methods. The predictor stage uses the method of characteristics to reconstruct the numerical fluxes whereas, the corrector stage recovers the conservation equations.

The proposed method is simple, conservative, non-oscillatory and suitable for multi-layer shallow water equations for which Riemann problems are difficult to solve. Numerical examples are presented to verify the considered multi-layer shallow water model. We demonstrate the model capability of calculating lateral and vertical distributions of velocities for wind-driven circulation over complex bathymetry.

The present paper is organized as follows. We first give a brief description of the model employed for multi-layer shallow water flows in section 2. In section 3, we then formulate the finite volume modified method of characteristics for the two-layer shallow water equations. This section includes the reconstruction of the numerical fluxes and the discretization of source terms. Numerical results are presented in section 4. Conclusions are summarized in section 5.

2 MULTI-LAYER SHALLOW WATER EQUATIONS

In the current study we are interested on hydraulic flows occurring on the water free-surface where assumptions of shallow water flows applied. We consider the one-dimensional multi-layer shallow water equations written in a conservative form as

$$\begin{aligned} \partial_t h_j + \partial_x \left(h_j u_j\right) &= 0, \qquad j = 1, \ldots, M, \\ \partial_t \left(h_j u_j\right) + \partial_x \left(h_j u_j^2 + \frac{1}{2} g h_j^2\right) &= -g h_j \partial_x \left(Z + \sum_{k=j+1}^{M} h_k + \sum_{k=1}^{j-1} \frac{\rho_k}{\rho_j} h_k\right) + \mathcal{F}_b + \mathcal{F}_w, \end{aligned} \tag{1}$$

where ρ_j is the water density of the jth layer, $h_j(t, x)$ is the water height of the jth layer, $u_j(t, x)$ is the local water velocity for the jth layer, $j = 1, \ldots, M$ with M is the total number of layers, $Z(x)$ is the bottom topography and g the gravitational acceleration. For more details on the derivation of the system (1) we refer to [5, 4, 6, 9] among others. Here, the water bodies $1, \ldots, M$ are labeled from top to bottom and

$$0 < \rho_1 \leq \cdots \leq \rho_M.$$

In the system (1), the bed friction forcing term $\mathcal{F}_b$ is acting only on the lower layer and the wind-driven forcing term $\mathcal{F}_w$ is acting only on the upper layer. They are given by

$$\mathcal{F}_b = -\delta_{Mj} \frac{\tau_b}{\rho_M}, \qquad \mathcal{F}_w = \delta_{1j} \frac{\tau_\omega}{\rho_1}, \tag{2}$$

with δ_{kj} represents the Kronecker delta, τ_b and τ_ω are respectively, the bed shear stress and the shear of the blowing wind defined by the water and wind velocities as

$$\tau_b = \rho_M C_b u_M \left|u_M\right|, \qquad \tau_\omega = \rho_1 C_\omega \omega |\omega|, \tag{3}$$

where C_b is the bed friction coefficient, which may be either constant or estimated as $C_b = g/C_z^2$, where $C_z = h_M^{1/6}/n_b$ is the Chezy constant, with n_b being the Manning

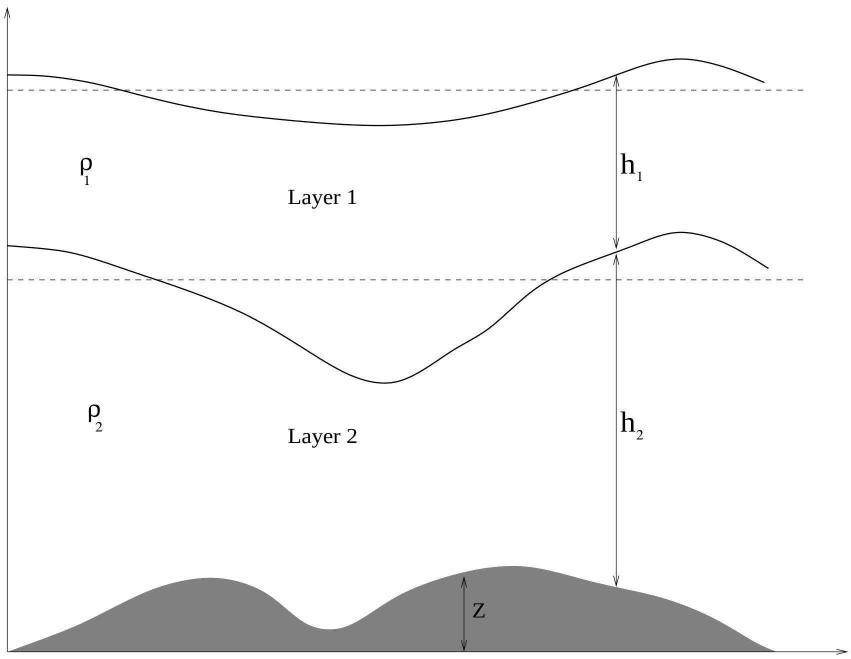

Figure 1: Schematic of a two-layer shallow water flow.

roughness coefficient at the bed, ω is the velocity of wind at 10 m above water surface and C_w is the coefficient of wind friction defined as [2]

$$C_w = \rho_a \left(0.75 + 0.067|\omega|\right) \times 10^{-3},$$

where ρ_a is the air density. It should be stressed that the multi-layer shallow water system admits a convex entropy [3] and at rest the system has the steady states

$$u_j = 0, \qquad \partial_x \left(Z + h_j + \sum_{k=j+1}^{M} h_k + \sum_{k=1}^{j-1} \frac{\rho_k}{\rho_j} h_k \right) = 0, \qquad j = 1, \ldots, M. \tag{4}$$

Note that if $\rho_1 < \cdots < \rho_M$, the condition (4) reduces to

$$u_j = 0, \qquad \partial_x \left(Z + h_M\right) = 0, \qquad \partial_x h_j = 0, \qquad j = 1, \ldots, M-1, \tag{5}$$

while if $\rho_1 = \cdots = \rho_M$, (4) reduces to

$$u_j = 0, \qquad \partial_x \left(Z + h_1 + \cdots + h_M\right) = 0. \tag{6}$$

In the present work, we formulate the finite volume modified method of characteristics for the one-dimensional two-layer hydraulic flows written in a conservative form as

$$
\begin{aligned}
\partial_t h_1 + \partial_x (h_1 u_1) &= 0, && \text{(7a)}\\
\partial_t (h_1 u_1) + \partial_x \left(h_1 u_1^2 + \frac{1}{2} g h_1^2 \right) &= -g h_1 \partial_x (Z + h_2) + \frac{\tau_\omega}{\rho_1}, && \text{(7b)}\\
\partial_t h_2 + \partial_x (h_2 u_2) &= 0, && \text{(7c)}\\
\partial_t (h_2 v_2) + \partial_x \left(h_2 u_2^2 + \frac{1}{2} g h_2^2 \right) &= -g h_2 \partial_x \left(Z + \frac{\rho_1}{\rho_2} h_1 \right) - \frac{\tau_b}{\rho_2}, && \text{(7d)}
\end{aligned}
$$

where the subscripts 1 and 2 represent respectively, the upper and lower layer in the hydraulic system, see the Figure 1 for an illustration. For simplicity in presentation we rewrite the equations (7) in a compact form as

$$
\partial_t \mathbf{W} + \partial_x \mathbf{F}(\mathbf{W}) = \mathbf{Q}(\mathbf{W}) + \mathbf{R}(\mathbf{W}), \tag{8}
$$

where $\mathbf{W}$ is the vector of conserved variables, $\mathbf{F}$ the vector of flux functions, $\mathbf{Q}$ and $\mathbf{R}$ are the vector of source terms

$$
\mathbf{W} = \begin{pmatrix} h_1 \\ h_1 u_1 \\ h_2 \\ h_1 u_2 \end{pmatrix}, \qquad \mathbf{F}(\mathbf{W}) = \begin{pmatrix} h_1 u_1 \\ h_1 u_1^2 + \frac{1}{2} g h_1^2 \\ h_2 u_2 \\ h_2 u_2^2 + \frac{1}{2} g h_2^2 \end{pmatrix},
$$

$$
\mathbf{Q}(\mathbf{W}) = \begin{pmatrix} 0 \\ -g h_1 \partial_x (Z + h_2) \\ 0 \\ -g h_2 \partial_x (Z + r h_1) \end{pmatrix}, \qquad \mathbf{R}(\mathbf{W}) = \begin{pmatrix} 0 \\ \frac{\tau_\omega}{\rho_1} \\ 0 \\ -\frac{\tau_b}{\rho_2} \end{pmatrix},
$$

where the ratio $r = \frac{\rho_1}{\rho_2}$. Notice that the equations (8) has to be solved in a bounded spatial domain with smooth boundary, equipped with given boundary and initial conditions. In practice, these conditions are problem dependent and their discussion is postponed for section 4 where numerical results are discussed.

3 FINITE VOLUME MODIFIED METHOD OF CHARACTERISTICS

It is well known that the calculation of the eigenvalues associated with the two-layer system (8) is not trivial. Indeed, the four eigenvalues λ_k $(k = 1, \ldots, 4)$ of the Jacobian $\frac{\partial \mathbf{F}}{\partial \mathbf{W}}$ are are the zeros of the characteristic polynomial [6]

$$P(\lambda) = \left(\lambda^2 - 2u_1\lambda + u_1^2 - gh_1\right)\left(\lambda^2 - 2u_2\lambda + u_2^2 - gh_2\right) - g^2 r h_1 h_2. \tag{9}$$

For oceanographic applications with $r \approx 1$ and $u_1 \approx u_2$, a first-order approximation of the eigenvalues can be obtained by expanding (9) in terms of $1 - r$ and $u_2 - u_1$ as

$$\begin{aligned}
\lambda_1 &\approx U_m - \sqrt{g\left(h_1 + h_2\right)}, \\
\lambda_2 &\approx U_m + \sqrt{g\left(h_1 + h_2\right)}, \\
\lambda_3 &\approx U_c - \sqrt{(1-r)g\frac{h_1h_2}{h_1+h_2}\left(1 - \frac{\left(u_2-u_1\right)^2}{(1-r)g\left(h_1+h_2\right)}\right)}, \\
\lambda_4 &\approx U_c + \sqrt{(1-r)g\frac{h_1h_2}{h_1+h_2}\left(1 - \frac{\left(u_2-u_1\right)^2}{(1-r)g\left(h_1+h_2\right)}\right)},
\end{aligned} \tag{10}$$

where

$$U_m = \frac{h_1u_1 + h_2u_2}{h_1 + h_2}, \qquad U_c = \frac{h_1u_2 + h_2u_1}{h_1 + h_2}.$$

It is evident that, depending on the values of the ratio r, the eigenvalues (10) may become complex. In this case, the system is not hyperbolic and yields to the so-called Kelvin-Helmholtz instability at the interface separating the two layers. A necessary condition for the system (8) to be hyperbolic is

$$\left(u_2 - u_1\right)^2 < (1 - r)g\left(h_1 + h_2\right). \tag{11}$$

It is worth remarking that the finite volume modified method of characteristics proposed in this paper does not require the calculation of the eigenvalues (10) and can be applied for arbitrary values of the ratio r. In this section we describe the different steps of the proposed finite volume modified method of characteristics.

3.1 Time integration procedure

Let us discretize the spatial domain into control volumes $[x_{i-1/2}, x_{i+1/2}]$ with uniform size $\Delta x = x_{i+1/2} - x_{i-1/2}$ and divide the temporal domain into subintervals $[t_n, t_{n+1}]$ with stepsize Δt. Here, $t_n = n\Delta t$, $x_{i-1/2} = i\Delta x$ and $x_i = (i + 1/2)\Delta x$ is the center of the

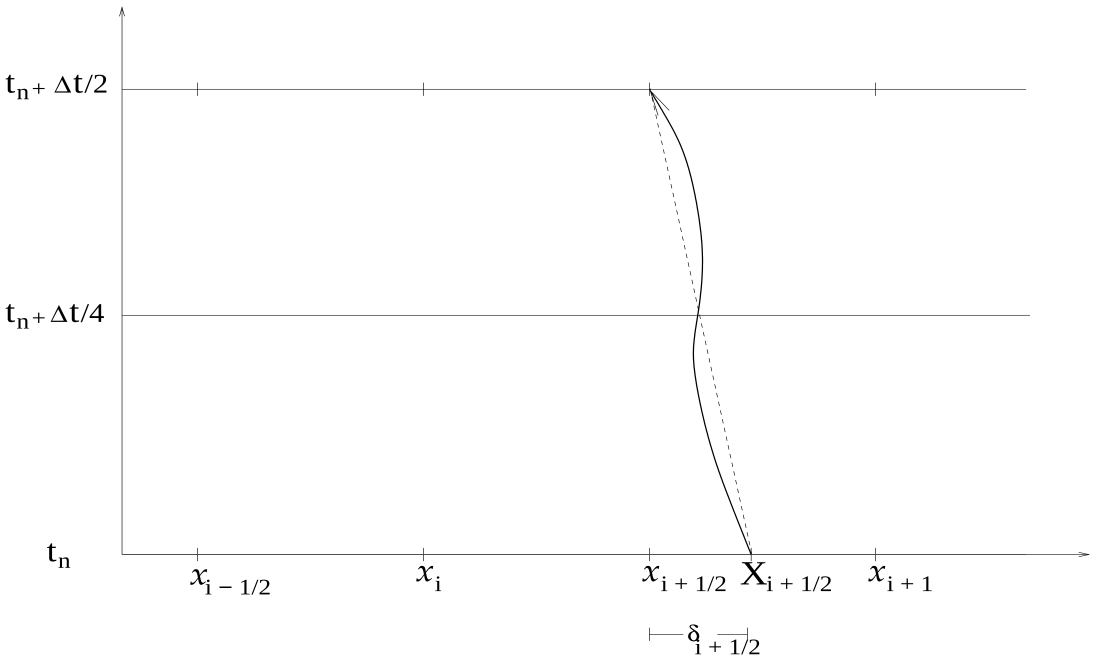

Figure 2: A schematic diagram showing the control volumes and the main quantities used in the calculation of the departure points. The exact trajectory is represented by a solid line and the approximate trajectory with a dashed line.

control volume. Integrating the equation (8) with respect to space over the control volume $[x_{i-1/2}, x_{i+1/2}]$ shown in Figure 2, we obtain the following semi-discrete equations

$$\frac{d\mathbf{W}_i}{dt} + \frac{\mathcal{F}_{i+1/2} - \mathcal{F}_{i-1/2}}{\Delta x} = \mathcal{Q}_i + \mathcal{R}_i, \tag{12}$$

where $\mathbf{W}_i(t)$ is the space average of the solution $\mathbf{W}$ in the control volume $[x_{i-1/2}, x_{i+1/2}]$ at time t, *i.e.*,

$$\mathbf{W}_i = \frac{1}{\Delta x}\int_{x_{i-1/2}}^{x_{i+1/2}} \mathbf{W}(t,x)\, dx,$$

and $\mathcal{F}_{i\pm1/2} = \mathbf{F}(\mathbf{W}_{i\pm1/2})$ are the numerical fluxes at $x = x_{i\pm1/2}$ and time t. In (12), $\mathcal{Q}_i$ and $\mathcal{R}_i$ are the difference notation for the discretized source terms $\mathbf{Q}(\mathbf{W}_i)$ and $\mathbf{S}(\mathbf{W}_i)$ in (8), respectively. To integrate the system (12) in time we consider an operator splitting method consisting first of the predictor step

$$\mathbf{W}_i^{n+1/2} = \mathbf{W}_i^n + \Delta t \mathcal{R}_i^n, \tag{13}$$

followed by the corrector step

$$\mathbf{W}_i^{n+1} = \mathbf{W}_i^{n+1/2} - \Delta t \frac{\mathcal{F}_{i+1/2}^{n+1/2} - \mathcal{F}_{i-1/2}^{n+1/2}}{\Delta x} + \Delta t \mathcal{Q}_i^{n+1/2}. \tag{14}$$

It should be pointed out that as with all explicit time stepping methods the theoretical maximum stable time step Δt is specified according to the Courant-Friedrichs-Lwey (CFL) condition

$$\Delta t = Cr \frac{\Delta x}{\max\limits_{k=1,\ldots,4} \left(|\lambda_k^n|\right)}, \tag{15}$$

where Cr is a constant to be chosen less than unity. The spatial discretization of the equation (14) is complete when a numerical construction of the n umerical fluxes $\mathcal{F}_{i\pm1/2}^{n+1/2}$ and source terms $\mathcal{Q}_i^{n+1/2}$ is chosen. In general, the construction of the numerical fluxes requires a solution of Riemann problems at the interfaces $x_{i\pm1/2}$. From a computational viewpoint, this procedure is very demanding and may restrict the application of the method for which Riemann solutions are not available. Our objective in the present work is to present a class of finite volume modified method of characteristics (FVC) that are simple, easy to implement, and accurately solves the equations (8) without relying on a Riemann problem solver. This objective is reached by reformulating the system (8) in an advective form and integrating the obtained system along the characteristics defined by the water velocity.

3.2 Discretization of the flux gradients

To reconstruct the numerical fluxes $\mathcal{F}_{i\pm1/2}^{n}$ in (14), we consider the method of characteristics applied to the advective version of the system (8). In general, the advective form of the two-layer system (8) is built such that the non-conservative variables are transported with the same velocity field associated with each layer. Here, the two-layer shallow water equations (8) are reformulated in an advective form as

$$\begin{aligned} \partial_t \mathbf{U}_1 + u_1 \partial_x \mathbf{U}_1 &= \mathbf{S}_1, \\ \partial_1 \mathbf{U}_2 + u_2 \partial_x \mathbf{U}_2 &= \mathbf{S}_2, \end{aligned} \tag{16}$$

where

$$\mathbf{U}_1 = \begin{pmatrix} h_1 \\ u_1 \end{pmatrix}, \qquad \mathbf{S}_1 = \begin{pmatrix} -h_1 \partial_x u_1 \\ -g\partial_x \left(Z + h_1 + h_2\right) \end{pmatrix}, \tag{17}$$

$$\mathbf{U}_2 = \begin{pmatrix} h_2 \\ u_2 \end{pmatrix}, \qquad \mathbf{S}_2 = \begin{pmatrix} -h_2 \partial_x u_2 \\ -g\partial_x \left(Z + rh_1 + h_2\right) \end{pmatrix}. \tag{18}$$

The fundamental idea of the method of characteristics is to impose a regular grid at the new time level and to backtrack the flow trajectories to the previous time level. At the old time level, the quantities that are needed are evaluated by interpolation from their known values on a regular grid, for more discussions we refer the reader to [13, 11, 12] among others. Thus, the characteristic curves associated with the equation (16) are solutions of the initial-value problems

$$\begin{aligned} \frac{dX_{j,i+1/2}(\tau)}{d\tau} &= u_{j,i+1/2}\Big(\tau, X_{j,i+1/2}(\tau)\Big), \quad \tau \in [t_n, t_n + \Delta t/2], \\ X_{j,i+1/2}(t_n + \Delta t/2) &= x_{i+1/2}, \qquad j = 1, 2. \end{aligned} \tag{19}$$

Note that $X_{j,i+1/2}(\tau)$ is the departure point at time τ of a particle that will arrive at point $x_{i+1/2}$ in time $t_n + \Delta t/2$. The method of characteristics does not follow the flow particles forward in time, as the Lagrangian schemes do, instead it traces backward the position at time t_n of particles that will reach the points of a fixed mesh at time $t_n + \Delta t/2$. By doing so, the method avoids the grid distortion difficulties that the conventional Lagrangian schemes have, see for instance [13, 11]. The solutions of (19) can be expressed as

$$\begin{aligned} X_{j,i+1/2}(t_n) &= x_{i+1/2} - \int_{t_n}^{t_n+\Delta t/2} u_{j,i+1/2}\left(X_{j,i+1/2}(\tau)\right) d\tau, \\ &= x_{i+1/2} - \delta_{j,i+1/2}. \end{aligned} \tag{20}$$

To approximate the integral in (20), we used a method first proposed by [13] in the context of semi-Lagrangian schemes to integrate the weather prediction equations. Note that $\delta_{j,i+1/2}$ denotes the displacement between a mesh point on the new level, x_i, and the departure point of the trajectory to this point on the previous time level $X_{j,i+1/2}(t_n)$, *i.e.*

$$\delta_{j,i+1/2} = x_{i+1/2} - X_{j,i+1/2}(t_n).$$

Applying the mid-point rule to approximate the integral in (20) yields

$$\delta_{j,i+1/2} = \frac{\Delta t}{2} u_{j,i+1/2}\left(t_{n+1/2}, X_{j,i+1/2}(t_{n+1/2})\right). \tag{21}$$

Using the second-order extrapolation

$$u_{j,i+1/2}(t_{n+1/2}, x_{i+1/2}) = \frac{3}{2} u_{j,i+1/2}(t_n, x_{i+1/2}) - \frac{1}{2} u_{j,i+1/2}(t_{n-1}, x_{i+1/2}), \tag{22}$$

and the second-order approximation

$$X_{j,i+1/2}(t_{n+1/2}) = x_{i+1/2} - \frac{1}{2}\delta_{j,i+1/2},$$

we obtain the following implicit formula for $\delta_{j,i+1/2}$

$$\delta_{j,i+1/2} = \frac{\Delta t}{2}\left[\frac{3}{2} u_{j,i+1/2}\left(t_n, x_{i+1/2} - \frac{1}{2}\delta_{j,i+1/2}\right) - \frac{1}{2} u_{j,i+1/2}\left(t_{n-1}, x_{i+1/2} - \frac{1}{2}\delta_{j,i+1/2}\right)\right].$$

To compute $\delta_{j,i+1/2}$ we consider the following successive iteration procedure:

$$\begin{aligned}
\delta^{(0)}_{j,i+1/2} &= \frac{\Delta t}{2}\left[\frac{3}{2}u_{j,i+1/2}\left(t_n, x_{i+1/2}\right) - \frac{1}{2}u_{j,i+1/2}\left(t_{n-1}, x_{i+1/2}\right)\right], \\
\delta^{(m)}_{j,i+1/2} &= \frac{\Delta t}{2}\left[\frac{3}{2}u_{j,i+1/2}\left(t_n, x_{i+1/2}\frac{1}{2}\delta^{(m-1)}_{j,i+1/2}\right)\right] \\
&\quad -\Delta t\left[\frac{1}{2}u_{j,i+1/2}\left(t_{n-1}, x_{i+1/2} - \frac{1}{2}\delta^{(m-1)}_{j,i+1/2}\right)\right], \qquad m = 1, 2, \ldots.
\end{aligned} \tag{23}$$

The iterations (23) are terminated when the following criteria

$$\frac{\left\|\delta^{(m)}_j - \delta^{(m-1)}_j\right\|}{\left\|\delta^{(m-1)}_j\right\|} < \varepsilon, \tag{24}$$

is fulfilled for the L^∞-norm $\|\cdot\|$ and a given tolerance ε. It is also known [10] that

$$\left\|\delta_j - \delta^{(m)}_j\right\| \leq \frac{\Delta t}{8}\left\|\delta_j - \delta^{(m-1)}_j\right\| \max\left(|u_1|, |u_2|\right), \qquad m = 1, 2, \ldots. \tag{25}$$

Hence, a necessary condition for the convergence of iterations (23) is that the velocity gradient satisfies

$$\max\left(|u_1|, |u_2|\right)\Delta t < 1. \tag{26}$$

Note that the condition (26) is sufficient to guarantee that the characteristics curves do not intersect during a time step of size $\Delta t/2$. A schematic representation of the quantities involved in computing the departure points is shown in Figure 2.

Once the characteristics curves $X_{j,i+1/2}(t_n)$ are known, a solution at the cell interface $x_{i+1/2}$ is reconstructed as

$$\mathbf{U}^n_{j,i+1/2} = \mathbf{U}_j\left(t_n + \Delta t/2, x_{i+1/2}\right) = \tilde{\mathbf{U}}_j\left(t_n, X_{j,i+1/2}(t_n)\right), \tag{27}$$

where $\tilde{\mathbf{U}}_j\left(t_n, X_{j,i+1/2}(t_n)\right)$ is the solution at the characteristic foot computed by interpolation from the gridpoints of the control volume where the departure point resides *i.e.*

$$\tilde{\mathbf{U}}_j\left(t_n, X_{j,i+1/2}(t_n)\right) = \mathcal{P}\Big(\mathbf{U}_j\left(t_n, X_{j,i+1/2}(t_n)\right)\Big), \tag{28}$$

where $\mathcal{P}$ represents the interpolating polynomial. For instance, a Lagrange-based interpolation polynomials can be formulated as

$$\mathcal{P}\Big(\mathbf{U}_j\left(t_n, X_{i+1/2}(t_n)\right)\Big) = \sum_k l_k(X_{j,i+1/2})\mathbf{U}^n_{j,k}, \tag{29}$$

with l_k are the Lagrange basis polynomials given by

$$l_k(x) = \prod_{\substack{q=0\\ q\neq k}} \frac{x - x_q}{x_k - x_q}.$$

Note that other interpolation procedures in (28) can also be applied.

3.3 Discretization of the source terms

Applied to the equations (16), the characteristic solutions are given by

$$\begin{aligned}
h^n_{1,i+1/2} &= \tilde{h}^n_{1,i+1/2} - \frac{\nu}{2}\tilde{h}^n_{1,i+1/2}\left(u^n_{1,i+1} - u^n_{1,i}\right),\\
u^n_{1,i+1/2} &= \tilde{u}^n_{1,i+1/2} - \frac{\nu}{2}g\left((Z + h^n_1 + h^n_2)_{i+1} - (Z + h^n_1 + h^n_2)_i\right),\\
h^n_{2,i+1/2} &= \tilde{h}^n_{2,i+1/2} - \frac{\nu}{2}\tilde{h}^n_{2,i+1/2}\left(u^n_{2,i+1} - u^n_{2,i}\right),\\
u^n_{2,i+1/2} &= \tilde{u}^n_{2,i+1/2} - \frac{\nu}{2}g\left((Z + rh^n_1 + h^n_2)_{i+1} - (Z + rh^n_1 + h^n_2)_i\right),
\end{aligned} \tag{30}$$

where $\nu = \frac{\Delta t}{\Delta x}$ and

$$\begin{aligned}
\tilde{h}^n_{1,i+1/2} &= h_1\left(t_n, X_{1,i+1/2}(t_n)\right), \qquad \tilde{u}^n_{1,i+1/2} = u_1\left(t_n, X_{1,i+1/2}(t_n)\right),\\
\tilde{h}^n_{2,i+1/2} &= h_2\left(t_n, X_{2,i+1/2}(t_n)\right), \qquad \tilde{u}^n_{2,i+1/2} = u_2\left(t_n, X_{2,i+1/2}(t_n)\right),
\end{aligned}$$

are the solutions at the characteristic foot computed by interpolation from the gridpoints of the control volume where the departure points $X_{1,i+1/2}(t_n)$ and $X_{2,i+1/2}(t_n)$ belong. The numerical fluxes $\mathcal{F}_{i\pm1/2}$ in (12) are calculated using the intermediate states $\mathbf{W}^n_{i\pm1/2}$ recovered accordingly from the characteristic solutions $\mathbf{U}^n_{j,i\pm1/2}$ in (27). Hence, the FVC method (14) reduces to

$$\begin{aligned}
h^{n+1}_{1,i} &= h^n_{1,i} - \nu\left((h_1u_1)^n_{i+1/2} - (h_1u_1)^n_{i-1/2}\right),\\
q^{n+1}_{1,i} &= q^n_{1,i} - \nu\left(\left(h_1u_1^2 + \frac{1}{2}gh_1^2\right)^n_{i+1/2} - \left(h_1u_1^2 + \frac{1}{2}gh_1^2\right)^n_{i-1/2}\right)\\
&\quad -\frac{1}{2}\nu g\hat{h}^n_{1,i}\left((Z + h_2)_{i+1} - (Z + h_2)_{i-1}\right),\\
h^{n+1}_{2,i} &= h^n_{2,i} - \nu\left((h_2u_2)^n_{i+1/2} - (h_2u_2)^n_{i-1/2}\right),\\
q^{n+1}_{2,i} &= q^n_{2,i} - \nu\left(\left(h_2u_2^2 + \frac{1}{2}gh_2^2\right)^n_{i+1/2} - \left(h_2u_2^2 + \frac{1}{2}gh_2^2\right)^n_{i-1/2}\right)\\
&\quad -\frac{1}{2}\nu g\hat{h}^n_{2,i}\left((Z + rh_1)_{i+1} - (Z + rh_1)_{i-1}\right),
\end{aligned} \tag{31}$$

where $q_1 = h_1u_1$ and $q_2 = h_2u_2$ are the water discharge associated with upper layer and lower layer, respectively. In our FVC method, the reconstruction of the term $\hat{h}^n_{1,i}$ and $\hat{h}^n_{2,i}$ in (31) is carried out such that the discretization of the source terms is well balanced with the discretization of flux gradients using the concept of C-property [2]. Here, a numerical scheme is said to satisfy the C-property for the equations (8) if the condition

$$u_1^n = u_2^n = 0, \qquad h_1^n = C_1 = constant, \qquad Z + h_2^n = C_2 = constant, \tag{32}$$

holds for stationary flows at rest. Therefore, the treatment of source terms in (31) is reconstructed such that the condition (32) is preserved at the discrete level.

Let us assume a stationary flow at rest, $u_1 = u_2 = 0$ and a linear interpolation procedure is used in the FVC method. Thus, the system (8) reduces to

$$\partial_t \begin{pmatrix} h_1 \\ 0 \\ h_2 \\ 0 \end{pmatrix} + \partial_x \begin{pmatrix} 0 \\ \frac{1}{2} g h_1^2 \\ 0 \\ \frac{1}{2} g h_2^2 \end{pmatrix} = \begin{pmatrix} 0 \\ -g h_1 \partial_x (Z + h_2) \\ 0 \\ -g h_2 \partial_x (Z + r h_1) \end{pmatrix}. \tag{33}$$

Applied to the system (33), the stage (30) computes

$$\begin{aligned} h_{1,i+1/2}^n &= \frac{h_{1,i}^n + h_{1,i+1}^n}{2}, \\ u_{1,i+1/2}^n &= 0, \\ h_{2,i+1/2}^n &= \frac{h_{2,i}^n + h_{2,i+1}^n}{2}, \\ u_{2,i+1/2}^n &= 0, \end{aligned} \tag{34}$$

while the stage (31) updates the solution as

$$\begin{aligned} h_{1,i}^{n+1} &= h_{1,i}^n, \\ q_{1,i}^{n+1} &= q_{1,i}^n - \frac{1}{2}\nu g \left(\left(h_{1,i+1/2}^n\right)^2 - \left(h_{1,i-1/2}^n\right)^2 \right) - \Delta t g \Big(h_1 \partial_x (Z + h_2) \Big)_i^n, \\ h_{2,i}^{n+1} &= h_{2,i}^n, \\ q_{2,i}^{n+1} &= q_{2,i}^n - \frac{1}{2}\nu g \left(\left(h_{2,i+1/2}^n\right)^2 - \left(h_{2,i-1/2}^n\right)^2 \right) - \Delta t g \Big(h_2 \partial_x (Z + r h_1) \Big)_i^n. \end{aligned} \tag{35}$$

To obtain stationary solutions $h_{1,i}^{n+1} = h_{1,i}^n$ and $h_{2,i}^{n+1} = h_{2,i}^n$, the sum of discretized flux gradient and source term in (35) should be equal to zero *i.e.*,

$$\begin{aligned} \frac{1}{2\Delta x} \left(\left(h_{1,i+1/2}^n\right)^2 - \left(h_{1,i-1/2}^n\right)^2 \right) &= -\Big(h_1 \partial_x (Z + h_2) \Big)_i^n, \\ \frac{1}{2\Delta x} \left(\left(h_{2,i+1/2}^n\right)^2 - \left(h_{2,i-1/2}^n\right)^2 \right) &= -\Big(h_2 \partial_x (Z + r h_1) \Big)_i^n. \end{aligned} \tag{36}$$

Using $h^n_{1,i+1/2} = \frac{h^n_{1,i}+h^n_{1,i+1}}{2}$ and $h^n_{2,i+1/2} = \frac{h^n_{2,i}+h^n_{2,i+1}}{2}$, the condition (36) is equivalent to

$$\begin{aligned}
\frac{1}{8\Delta x}\left(h^n_{1,i+1}+2h^n_{1,i}+h^n_{1,i-1}\right)\left(h^n_{1,i+1}-h^n_{1,i-1}\right) &= -\Big(h_1\partial_x\left(Z+h_2\right)\Big)^n_i,\\
\frac{1}{8\Delta x}\left(h^n_{2,i+1}+2h^n_{2,i}+h^n_{2,i-1}\right)\left(h^n_{2,i+1}-h^n_{2,i-1}\right) &= -\Big(h_2\partial_x\left(Z+rh_1\right)\Big)^n_i.
\end{aligned}\tag{37}$$

Since for stationary solutions $h^n_{1,i+1}-h^n_{1,i-1} = Z_{i+1}-Z_{i-1}$ and $h^n_{2,i+1}-h^n_{2,i-1} = Z_{i+1}-Z_{i-1}$, the equations (37) become

$$\begin{aligned}
\Big(h_1\partial_x\left(Z+h_2\right)\Big)^n_i &= \frac{h^n_{1,i+1/2}+h^n_{1,i-1/2}}{2}\,\frac{(Z+h_2)^n_{i+1}-(Z+h_2)^n_{i-1}}{2\Delta x},\\
\Big(h_2\partial_x\left(Z+rh_1\right)\Big)^n_i &= \frac{h^n_{2,i+1/2}+h^n_{2,i-1/2}}{2}\,\frac{(Z+rh_1)^n_{i+1}-(Z+rh_1)^n_{i-1}}{2\Delta x}.
\end{aligned}\tag{38}$$

Hence, if the source terms $\hat{h}^n_{1,i}$ and $\hat{h}^n_{2,i}$ in the stage of (31) are discretized as

$$\begin{aligned}
\hat{h}^n_{1,i} &= \frac{1}{4}\left(h^n_{1,i+1}+2h^n_{1,i}+h^n_{1,i-1}\right),\\
\hat{h}^n_{2,i} &= \frac{1}{4}\left(h^n_{2,i+1}+2h^n_{2,i}+h^n_{2,i-1}\right),
\end{aligned}\tag{39}$$

then the proposed FVC method satisfies the C-property. A detailed analysis of convergence and stability has been presented in [1] for nonlinear scalar problems. Notice that this property is achieved by assuming a linear interpolation procedure in the predictor stage of the FVC method. However, a well-balanced discretization of flux gradients and source terms for a quadratic or cubic interpolation procedures can be carried out using similar techniques.

In summary, the implementation of FVC algorithm to solve the two-layer shallow water equations (8) is carried out in the following steps. Given $\left(h^n_{1,i}, q^n_{1,i}, h^n_{2,i}, q^n_{2,i}\right)$, we compute $\left(h^{n+1}_{1,i}, q^{n+1}_{1,i}, h^{n+1}_{2,i}, q^{n+1}_{2,i}\right)$ via:

Step 1. *Compute the departure points $X_{1,i+1/2}(t_n)$ and $X_{2,i+1/2}(t_n)$ using the iterative procedure* (23).

Step 2. *Compute the approximations*

$$\tilde{h}^n_{1,i+1/2} = h_1\left(t_n, X_{1,i+1/2}(t_n)\right), \qquad \tilde{u}^n_{1,i+1/2} = u_1\left(t_n, X_{1,i+1/2}(t_n)\right),$$

$$\tilde{h}^n_{2,i+1/2} = h_2\left(t_n, X_{2,i+1/2}(t_n)\right) \quad \textit{and} \quad \tilde{u}^n_{2,i+1/2} = u_2\left(t_n, X_{2,i+1/2}(t_n)\right),$$

employing an interpolation procedure.

Table 1: Reference parameters used for two-layer wind-driven flow problem.

Quantity	Reference value
ρ_1	$990\ kg/m^3$
ρ_2	$1100\ kg/m^3$
ρ_a	$1.2\ kg/m^3$
g	$9.81\ m/s^2$
n_b	$0.035\ s/m^{1/3}$

Step 3. *Evaluate the intermediate states* $h^n_{1,i+1/2}$, $u^n_{1,i+1/2}$, $h^n_{2,i+1/2}$ *and* $u^n_{2,i+1/2}$ *from the predictor stage* (30).

Step 4. *Update the solutions* $h^{n+1}_{1,i}$, $q^{n+1}_{1,i}$, $h^{n+1}_{2,i}$ *and* $q^{n+1}_{2,i}$ *using the corrector stage* (31).

Note that other interpolation procedures in Step 2 can also be applied. In our simulations we have used a linear interpolation since for this type of interpolations the obtained solution remains monotone and the FVC method preserves the exact C-property at the machine precision, compare [1].

REMARK **1** *In order to avoid the division by very small values of* h_1 *and* h_2 *in the computation of the velocities* u_1 *and* u_2*, we use the following formula [8]*

$$u_j = \frac{\sqrt{2}h_j q_j}{\sqrt{h_j^4 + \max\left(\xi, h_j^4\right)}}, \qquad j = 1, 2, \tag{40}$$

where ξ *is a perturbation number selected a-priori. In our computations presented in this study,* $\xi = \Delta x$.

It is evident that, for large values of h_j, the formula (40) reduces to $u_j = q_j/h_j$, $j = 1, 2$.

4 NUMERICAL RESULTS

To examine the performance of the proposed FVC method we consider a test example of two-layer wind-driven flow problem in a lake with non-flat topography. The lake is of length 2000 m and the bed consists of four bumps as

$$Z(x) = \sum_{k=1}^{4} A_k \exp\left(-\left(\frac{x - x_k}{100}\right)^2\right),$$

where $A_1 = A_3 = 0.5$, $A_2 = 1$, $A_4 = 0.25$, $x_1 = 500\ m$, $x_2 = 800\ m$, $x_3 = 1100\ m$ and $x_4 = 1400\ m$. Initial water levels and initial velocities are given as

$$h_2(0, x) = 7\ m - Z(x), \quad h_1(0, x) = 13\ m - h_2(0, x) - Z(x), \quad u_1(0, x) = u_2(0, x) = 0\ m/s.$$

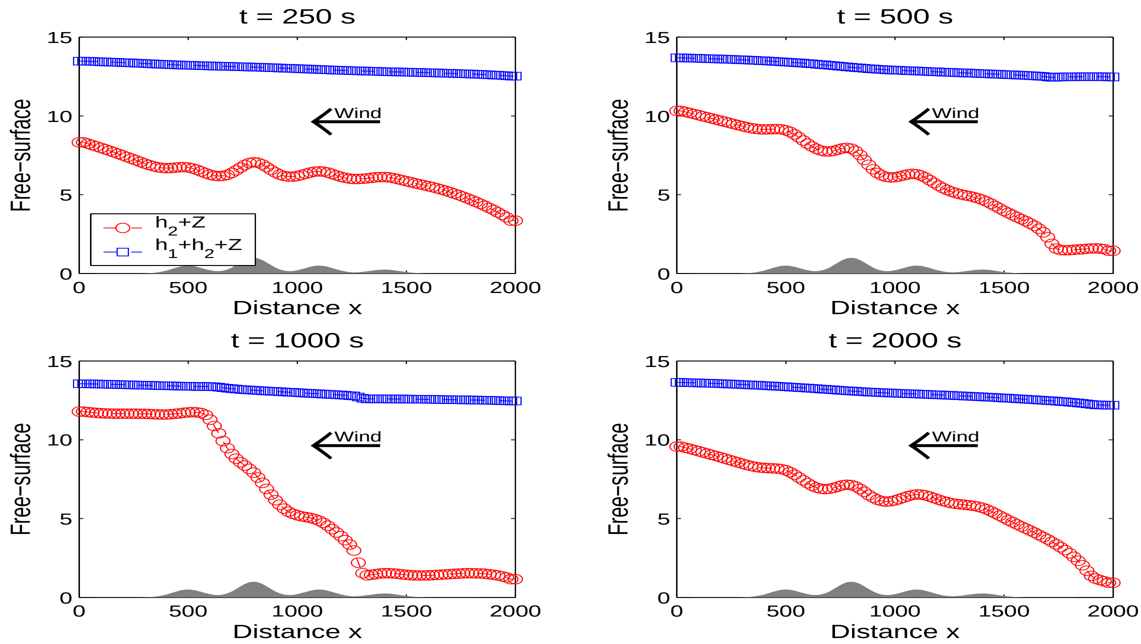

Figure 3: Water free-surface for blowing wind from the east at four simulation times.

The selected values for the evaluation of the present method are summarized in Table 1. Depending on the wind conditions, two situations are simulated namely:

(i) Wind blowing from the east corresponding to ($\omega = -5.1\ m/s$).

(ii) Wind blowing from the west corresponding to ($\omega = 5.1\ m/s$).

The computational domain is discretized in 100 gridpoints and the computed water free-surface and velocity fields are illustrated at four different instants $t = 250\ s$, $t = 500\ s$, $t = 1000\ s$ and $t = 2000\ s$. In all our computations a fixed courant number $Cr = 0.75$ is used while the time step is varied according to the stability condition (15).

In Figure 3 and Figure 4 we present numerical results for the water free-surface and the water velocity respectively, obtained using conditions for the wind blowing from the east. Those results obtained for the wind blowing from the west are displayed in Figure 5 and Figure 6. In Figure 3 and Figure 5, we also show the the topography used in the lake. It is clear that using the considered wind conditions in the two-layer shallow water flow example, the flow exhibits a hydraulic jump with different order of magnitudes near the center of the lake. At the beginning of simulation time, the water flow enters the lake from the eastern boundary and flows towards the eastern exit of the lake. At later time, due to wind effects, the water flow changes the direction pointing towards the eastern coast of the lake. Note that this recirculation features of the water flow can not be captured using the conventional single-layer shallow water equations. A periodic behavior is also detected

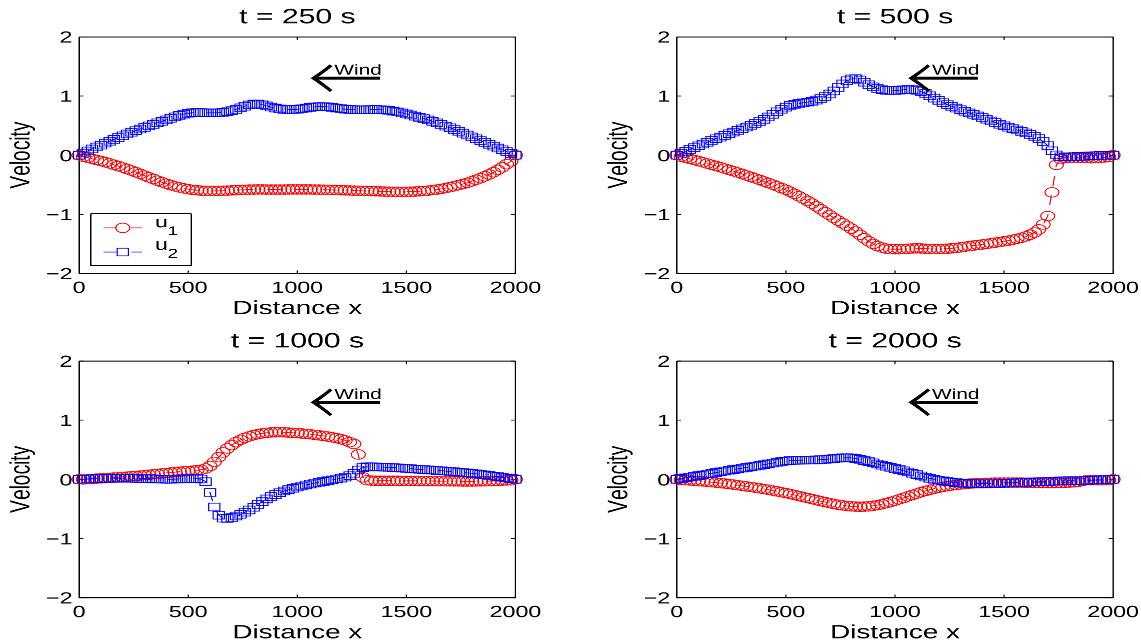

Figure 4: Water velocity for blowing wind from the east at four simulation times.

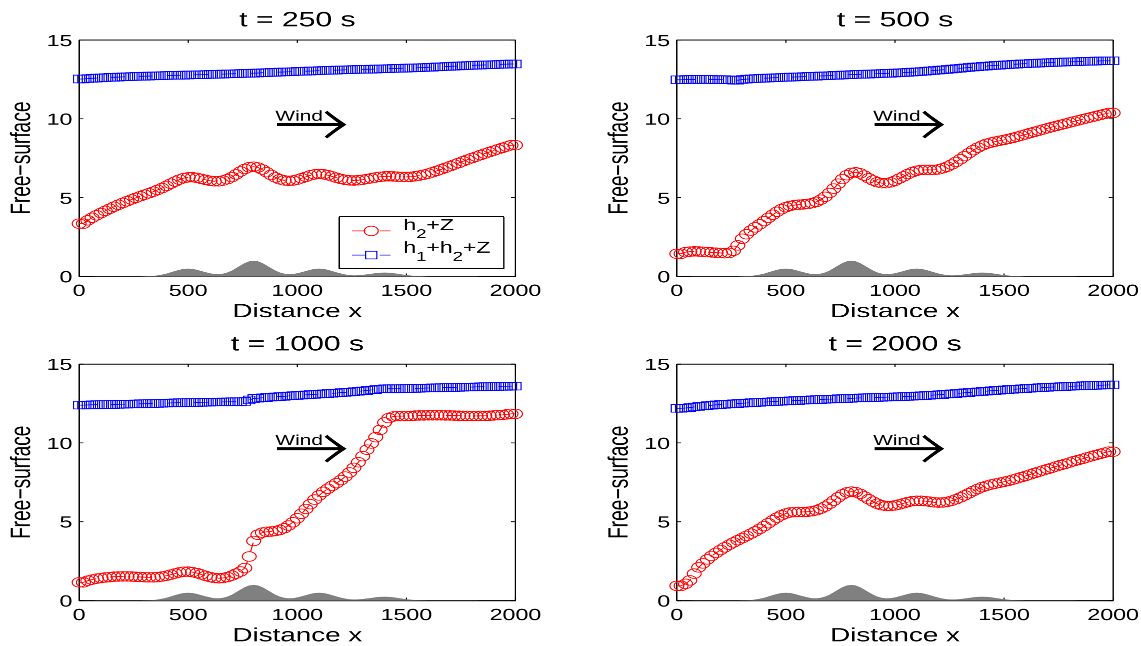

Figure 5: Water free-surface for blowing wind from the west at four simulation times.

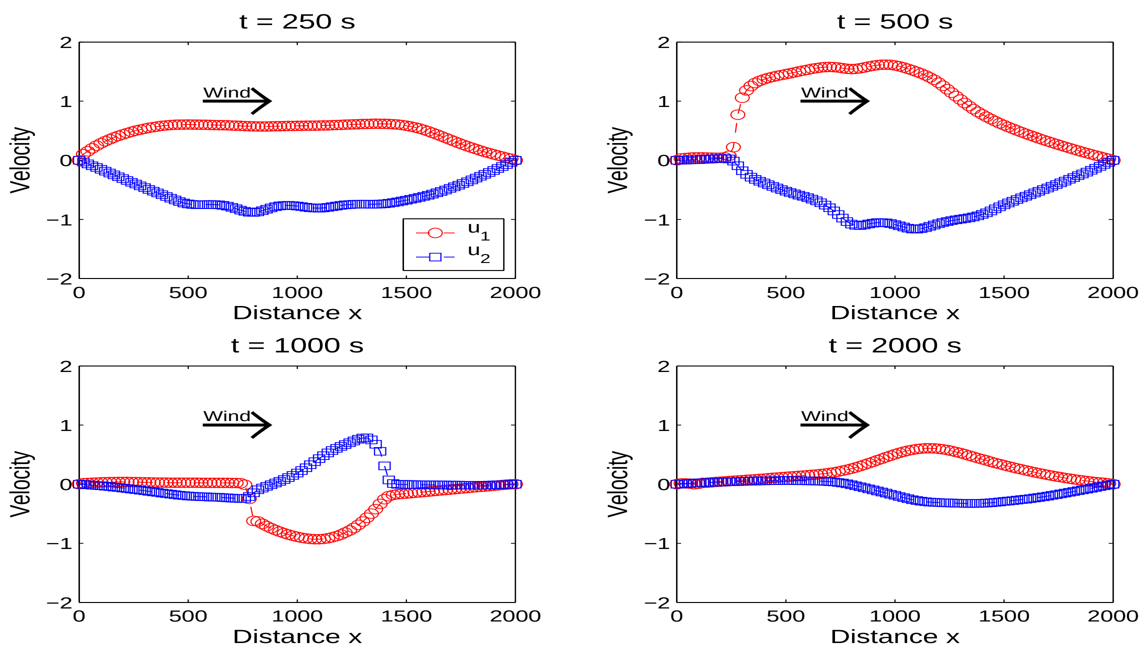

Figure 6: Water velocity for blowing wind from the west at four simulation times.

for the considered two-layer shallow water flow problem subject to the wind blowing from the east and west. The proposed FVC method performs very satisfactorily for this test problem since it does not diffuse the moving fronts and no spurious oscillations have been detected near steep gradients of the flow field in the computational domain. It should be stressed that the performance of the FVC method is very attractive since the computed solution remains stable and accurate even when coarse meshes are used without requiring Riemann-problem solvers or complicated techniques to balance the source terms and flux gradients.

5 CONCLUSIONS

In this paper we have proposed a simple and accurate finite volume modified method of characteristics to solve the multi-layer shallow water equations. A detailed formulation of the method has been presented for the special case of two-layer system. The method combines the attractive attributes of the finite volume discretization and the method of characteristics to yield a robust algorithm for multi-layer hydraulic flows. The new method can compute the numerical flux corresponding to the real state of water flow without relying on Riemann problem solvers. Furthermore, the proposed approach does not require either nonlinear solution or special front tracking techniques.

The proposed method has been numerically examined for the test example of two-layer wind driven flow problem on non-flat topography. The obtained results have exhibited accurate prediction of both, the free surface and the velocity field with correct C-property, and stable representation of free surface response to the lower layer. The results make it promising to be applicable also to real situations where, beyond the many sources of complexity, there is a more severe demand for accuracy in predicting multi-layer shallow water flows, which must be performed for long time.

Acknowledgment

Financial support provided by Mhycof, université Paris 13 is gratefully acknowledged.

REFERENCES

[1] F. Benkhaldoun and M. Seaïd, A simple finite volume method for the shallow water equations, *J. Comp. Applied Math.*, **234**, 58–72 (2010).

[2] A. Bermudez and M.E. Vázquez-Cendón, Upwind methods for hyperbolic conservation laws with source terms, *Computers & Fluids.*, **23**, 1049–1071 (1994).

[3] F. Bouchut and T. Morales, An entropy satisfying scheme for two-layer shallow water equations with uncoupled treatment, *M2AN Math. Model. Numer. Anal.*, **42**, 683–698 (2008).

[4] M.J. Castro, T. Chacón, E.D. Nieto and C. Parés, On well-balanced finite volume methods for nonconservative nonhomogeneous hyperbolic systems, *SIAM J. Sci. Comput.*, **29**, 1093–1126 (2007).

[5] M.J. Castro, J.A. García-Rodrguez, J.M. González-Vida, J. Macías, C. Parés and M.E. Vázquez-Cendón, Numerical simulation of two-layer shallow water flows through channels with irregular geometry, *J. Comp. Physics.*, **195**, 202–235 (2004).

[6] M.J. Castro, J. Macías and C. Parés, A Q-scheme for a class of systems of coupled conservation laws with source term. Application to a two-layer 1D shallow water system, *M2AN Math. Model. Numer. Anal.*, **35**, 107–127 (2001).

[7] D. Farmer and L. Armi, Maximal two-layer exchange over a sill and through a combination of a sill and contraction with barotropic flow, *J. Fluid Mech.*, **164**, 53–76 (1986).

[8] A. Kurganov and G. Petrova, A second-order well-balanced positivity preserving central-upwind scheme for the Saint-Venant system, *Commun. Math. Sci.*, **5**, 133–160 (2007).

[9] J. Macías, C. Parés and M.J. Castro, Improvement and genralization of a finite element shallow water solver to multi-layer systems, *Int. J. Numer. Methods Fluids.*, **31**, 1037–1059 (1999).

[10] J. Pudykiewicz and A. Staniforth, Some properties and comparative performance of the semi-Lagrangian method of Robert in the solution of advection-diffusion equation, *Atmos. Ocean.*, **22**, 283–308 (1984).

[11] M. Seaïd, On the quasi-monotone modified method of characteristics for transport-diffusion problems with reactive sources, *Comp. Methods in App. Math.*, **2**, 186–210 (2002).

[12] M. Seaïd, Semi-Lagrangian integration schemes for viscous incompressible flows, *Comp. Methods in App. Math.*, **4**, 392–409 (2002).

[13] C. Temperton and A. Staniforth, An efficient two-time-level semi-Lagrangian semi-implicit integration scheme, *Quart. J. Roy. Meteor. Soc.*, **113**, 1025–1039 (1987).